Sunlight and marine weathering of poly(oxymethylene): Evolution of the physico-chemical properties

Lata Soccalingame, Maialen Palazot, Mikäel Kedzierski, Stéphane Bruzaud

▶ **To cite this version:**

Lata Soccalingame, Maialen Palazot, Mikäel Kedzierski, Stéphane Bruzaud. Sunlight and marine weathering of poly(oxymethylene): Evolution of the physico-chemical properties. Marine Pollution Bulletin, 2023, 193, pp.115070. ⟨10.1016/j.marpolbul.2023.115070⟩. ⟨hal-04535441⟩

HAL Id: hal-04535441

https://hal.science/hal-04535441v1

Submitted on 9 Jul 2025

HAL is a multi-disciplinary open access archive for the deposit and dissemination of scientific research documents, whether they are published or not. The documents may come from teaching and research institutions in France or abroad, or from public or private research centers.

L'archive ouverte pluridisciplinaire **HAL**, est destinée au dépôt et à la diffusion de documents scientifiques de niveau recherche, publiés ou non, émanant des établissements d'enseignement et de recherche français ou étrangers, des laboratoires publics ou privés.

Distributed under a Creative Commons CC BY-NC 4.0 - Attribution - Non-commercial use - International License

Version of Record: https://www.sciencedirect.com/science/article/pii/S0025326X23005027
Manuscript_6fce2b9aa242e2b82d97328c0b209965

Sunlight and marine weathering of poly(oxymethylene): evolution of the physico-chemical properties

Lata Soccalingame [a], Maialen Palazot [a], Mikäel Kedzierski [a], Stéphane Bruzaud [a]

[a] Université Bretagne Sud, UMR CNRS 6027, IRDL, F-56100 Lorient, France

Abstract:

Plastic pollution is now an environmental problem that affects all environmental compartments. The study of plastic degradation in terrestrial, marine and other freshwater environments is emerging. Research is mainly focused on plastic fragmentation into microplastics. In this contribution, an engineering polymer, poly(oxymethylene) (POM), was studied under different weathering conditions using physico-chemical characterization techniques. A POM homopolymer and a POM copolymer were characterized by electron microscopy, tensile tests, DSC, infrared spectroscopy and rheometry tests after climatic and marine weathering or artificial UV/water spray cycles. Natural climatic conditions were the most favorable for POM degradation, especially under solar UV, as evidenced by the strong fragmentation into microplastics when subjected to artificial UV cycles. The evolution of properties with exposure time was found to be non-linear under natural conditions, in contrast to artificial conditions. Two main stages of degradation were evidenced by the correlation between strain at break and carbonyl indices.

Keywords:

Polyoxymethylene, plastic pollution, photodegradation, marine weathering, solar weathering

1 Introduction

Plastic pollution has recently become a major research topic. Numerous papers have addressed its occurrence in the environment and its potential risk to harm ecosystems, aquatic and terrestrial organisms and human health [1]–[3]. The size of plastic particles and their degraded state are important parameters as they strongly influence their interactions with fauna and flora, but also with persistent organic pollutants (POPs) [4]–[6]. Most of the available data on the characterization of plastic pollution concerns macroplastic and mesoplastic litter (from a few cm to larger) as well as floating microplastics (generally from 300 µm to 5 mm in size). The most common polymers found in the environment are polyethylene, polypropylene and polystyrene, which are the most produced in the world [7], [8].

The poly(oxymethylene) (POM) is an engineering polymer used in automotive and various other technical parts (mechanical gears or fastener assemblies for instance). The thermal degradation of POM was studied extensively in the 1960s and more sporadically later, so its degradation mechanisms under thermo-oxidative conditions are well known [9]–[15]. Investigations on the effects of light irradiation are less common in literature, but the photo-oxidation mechanisms of POM are also well documented by the community [16]–[18]. For certain demanding applications, POM is a judicious choice due to its good physical and mechanical

© 2023 published by Elsevier. This manuscript is made available under the CC BY NC user license
https://creativecommons.org/licenses/by-nc/4.0/

properties compared to other engineering resins such as polyamides, polycarbonates or styrene plastics. However, POM is known to release gaseous degradation products under thermo-oxidative or photo-oxidative conditions. Among these compounds, formaldehyde, depending on its concentration, could be a major source of toxicity. Therefore, it appears necessary to investigate the influence of copolymerization on POM weathering. From a microplastic pollution perspective, only one paper has dealt with the fragmentation of POM (pellets) under terrestrial and marine conditions. This study from Tang et al. observed a strong fragmentation phenomenon after 3 years under natural sunlight, producing 100-300µm particles [19].

In this study, the objective is to monitor the physical and chemical behavior of poly(oxymethylene) under artificial and natural weathering conditions for up to 18 months. Comparing the influence of these conditions on POM allows a better understanding of how POM plastic waste might evolve in the environment, depending on the degradation factors to which it has been subjected. POM homopolymer and copolymer are compared using electron microscopy, tensile tests, DSC, infrared spectroscopy and rheometry tests.

2 Materials & Methods

2.1 Materials

The polyoxymethylene (POM) references are supplied by Asahi Kasei: one is a homopolymer POM-H (POM Tenac Z4060) and the second one is a copolymer POM-C (POM Tenac HC550). According to the technical datasheet, POM Z4060 has a density of 1.42 $g.cm^{-3}$ and a MFR of 17 $g.10min^{-1}$ (melt mass-flow rate at 190°C/2.16 kg). POM HC550 has a density of 1.41 $g.cm^{-3}$ and a MFR of 15 $g.10min^{-1}$. Heat-stabilizing or UV-stabilizing additives were not indicated by the supplier. Samples are 800 µm-thick injected plates from these two polymers with dimensions of 78 mm x 29 mm. Tensile tests are carried out on normalized dog-bone samples (1BA geometry, ISO 527-2) obtained from machining the injected plates for the natural weathering. They were laser-cut for the artificial weathering set of samples, hence different initial mechanical properties.

2.2 Weathering conditions

2.2.1 Natural weathering

Samples were exposed to two types of natural weathering for 18 months: under outdoor climatic conditions and immersed in seawater. The outdoor climatic conditions were obtained on a rooftop in Lorient, France (GPS coordinates: 47.7474; -3.3955), allowing the samples to be exposed to natural sunlight and precipitations outdoor. The exposure lasted from July 2019 to February 2021. This location has an oceanic climate and is classified Cfb in the Köppen-Geiger classification: warm temperate climate without dry season with temperate summer. Samples were clipped in metallic fixations at about 20 cm above the ground and

oriented to the south. Plastic racks structure the whole setup and were drilled to avoid rain water accumulation.

Figure 1 – Climatic weathering installation on the Lorient rooftop

Samples were immersed at the Kernevel harbor in Larmor-Plage, France (GPS coordinates: 47.7173, −3.3666) from June 2020 to December 2021. Over a year, the average seawater temperature is 13°C (min 7°C, max 24°C). Injected plates of the studied polymers were contained in closed fishing nets attached underneath a pier (Figure 1). The nets were always between 2 m and 3 m deep and distance to the seafloor varied between 1 m to 7 m depending on the tide [20].

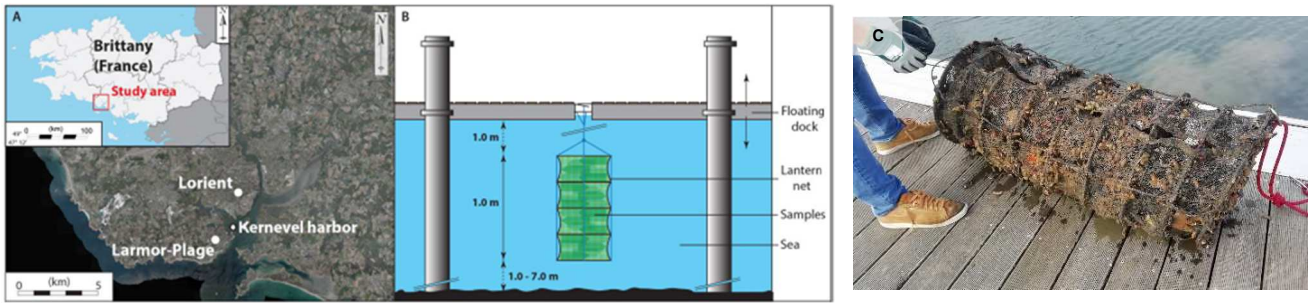

Figure 2 - A) Localization of the Kernevel harbor in the Lorient Bay, B) scheme of net installation [20], C) net condition after several months spent under the pier

To remove biofilm from submerged plastic samples, they were soaked in a potassium hydroxide solution (KOH 10%) for 24 hours, then rinsed with fresh water and gently wiped with a paper towel. Characterization methods were carried out afterward.

2.2.2 Artificial accelerated UV weathering

The artificial UV conditions were applied for up to 3 weeks in a QUV weathering chamber from QLab. The ISO 4892 standard was used; these cycles were repeated several times to achieve the desired sampling time: 8h of constant UV exposure at 0.76 $W.m^{-2}.nm^{-1}$ followed by 15 min of distilled water spray then 3h45 of condensation (humid atmosphere with water condensation on surfaces) . The whole weathering is regulated at 50°C.

2.3 Characterization techniques

2.3.1 Scanning Electron microscopy (SEM)

Microscopy analyses were performed with a Jeol JS-IT500-HR scanning electron microscope (SEM) to examine the surface of POM samples. Samples were carbon-coated before examination.

2.3.2 Tensile tests

Uniaxial tensile tests were carried out in an environmentally controlled laboratory, according to ISO 527 (23 °C and 50% relative humidity) on an MTS Criterion Model 42 testing machine. To determine the Young modulus, the loading speed was 1 mm.min^{-1} and an MTS extensometer was used to measure strain over a 25-mm gauge length. Ultimate strength, strength at break and strain at break were measured at a loading rate of 20 mm.min^{-1}. Five specimens were tested for each sampling, and the results were averaged.

2.3.3 Differential Scanning Calorimetry (DSC)

To assess the evolution of the POM microstructure under the different weathering conditions, differential scanning calorimetry (DSC) analyses were carried out on samples of approximately 10 mg, in 40-µL standard aluminum pans, using a Mettler-Toledo DSC3 equipment under a nitrogen atmosphere. The samples were heated from 25 to 200 °C and kept at 200 °C for 3 min. The samples were then cooled to 25 °C and finally a second heating scan from 25 to 200 °C was applied. The heating and cooling rates were 10 °C.min^{-1}. The degree of crystallinity $\%_{cr}$ was determined by the following equation (2):

$$\%_{\mathrm{cr}} = \frac{\Delta Hm_{exp}}{\Delta Hm_{100\%}} \times 100 \quad (2)$$

Where ΔHm_{exp} (J.g^{-1}) is the melting enthalpy of the sample. $\Delta Hm_{100\%}$ is the melting enthalpy for a 100% crystalline POM, taken to be 236.7 J.g^{-1} [11].

2.3.4 Infrared spectroscopy (FTIR-ATR)

Spectra were acquired from the POM sample surface using an Attenuated Total Reflection Fourier Transform Infrared spectrometer (ATR-FTIR Vertex70V, Bruker). All spectra were recorded in absorbance mode in the 4,000-600 cm^{-1} region with a 4 cm^{-1} resolution and 16 scans. Each POM sample was placed on the germanium diamond cell (ATR Golden Gate). To evaluate the oxidation state of the POM samples, carbonyl indices CI were calculated using the following equation (1):

$$\text{Carbonyl index (CI)} = \frac{\mathrm{A}_{[1780\text{-}1710]}}{\mathrm{A}_{[1515\text{-}1450]}} \quad (1)$$

$A_{[1780\text{-}1710]}$ is the spectrum area between 1780 and 1710 cm^{-1}, corresponding to the carbonyl bond from the aldehyde group (-C=O) centered at 1733 cm^{-1}. $A_{[1515\text{-}1450]}$ is the spectrum area between 1515 and 1450 cm^{-1}, corresponding to the methylene group (-CH_2) centered at 1470 cm^{-1} (cf. Figure 2). This methylene group is considered as the reference to monitored the carbonyl yields during the weathering [12].

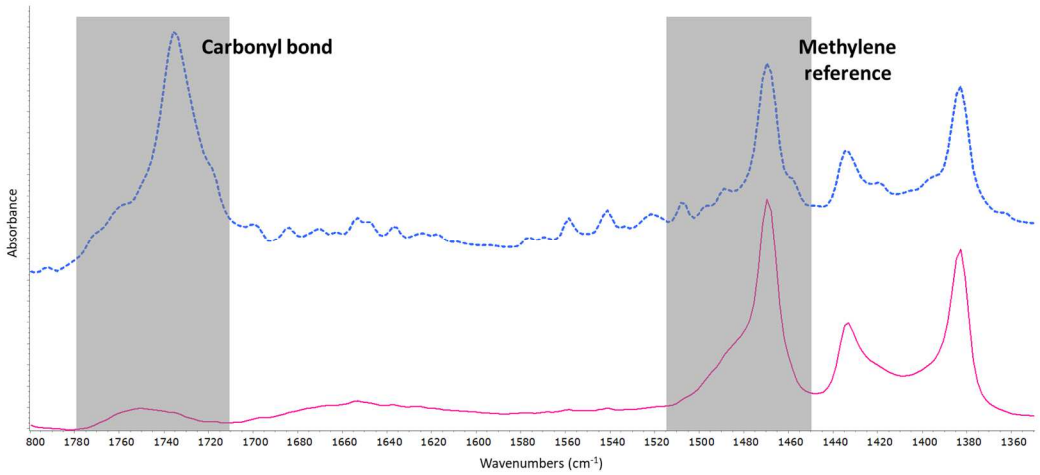

Figure 3 – Example of homopolymer POM spectra before (in pink solid line) and after artificial UV weathering (in blue dashed line)

2.3.5 Rheometry tests

Changes in POM molecular structure were assessed by melt viscoelasticity experiments in oscillatory shear mode using a rotational controlled strain rheometer (Anton Paar Physica MCR 301) equipped with a 25-mm diameter parallel plate geometry. All tests were carried out at a fixed temperature of 190°C under dry airflow. A strain amplitude within the linear viscoelastic region of 0,2% was applied. A frequency sweep from 0.1 to 100 Hz was performed.

3 Results & Discussion

3.1 Surface morphology

After 18 months under climatic conditions, a smooth surface was still observed on POM-H whereas cracks had appeared on POM-C with a spacing of 300 to 500 µm between cracks. For both POM references, 18 months in seawater did not induce any significant visual degradation except some scratches caused by living organisms found in the net (various species of urchins and crabs) (cf. Figure 3). Thus, POM-C was more sensitive to surface degradation under climatic conditions than POM-H.

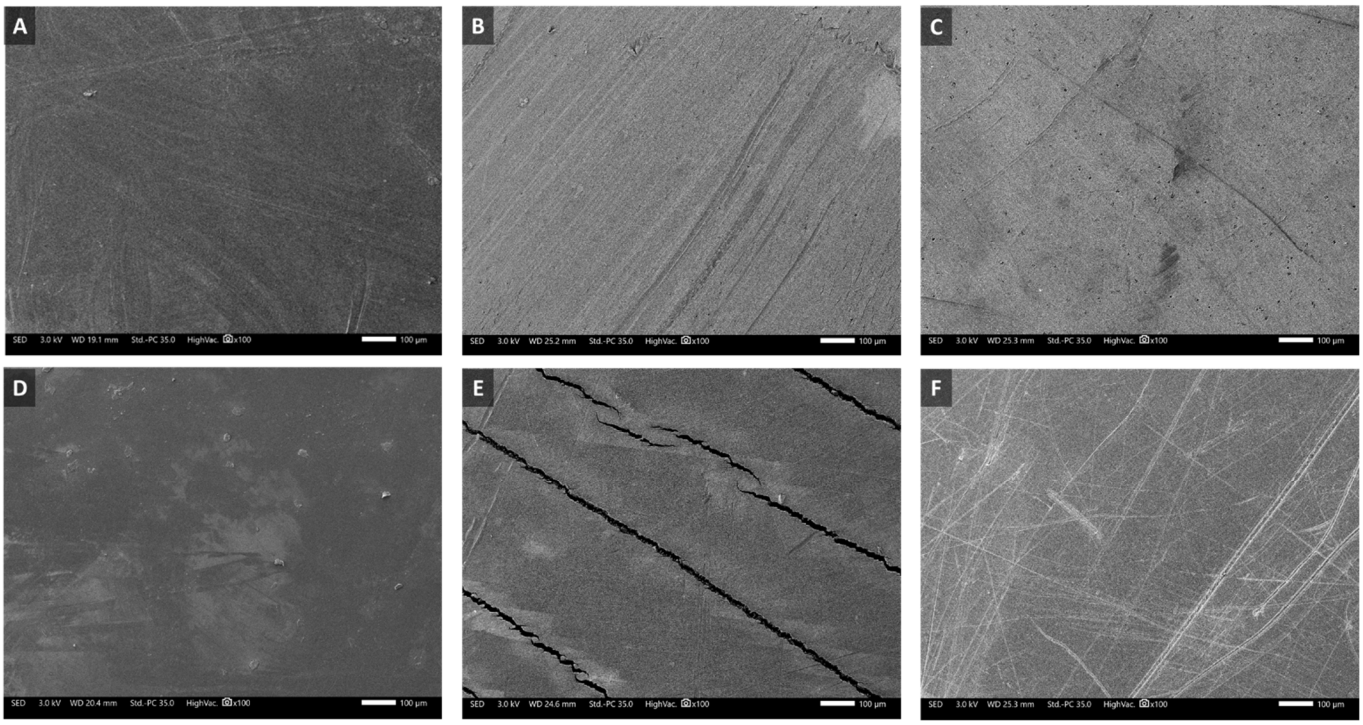

Figure 4 - Surface morphology under electron microscopy of POM-H (on the top-row) and POM-C (on the bottom-row) in the pristine state (A and D), after 18 months under outdoor climatic conditions (B and E) and submerged in seawater (C and F)

In a previous study by Tang et al., surface cracking was also observed on POM pellets after 1.5 years of exposure to sunlight in a tropical climate (Taiwan) [19]. Important striations were found with cracks separated by 100-200 µm, and fragments of material were also lost from the pellets.

Under accelerated artificial UV weathering, the degradation phenomenon is enhanced due to the harsher conditions. At a low magnification (x100), severe cracks were visible for both POM polymer after only one week of exposure (cf. Figure 4 and Figure 5). The larger cracks were separated by a distance of 150 to 250 µm. Finer cracks also appeared after one week and increased in size over time, leading to a spacing of 50 to 100 µm between the cracks.

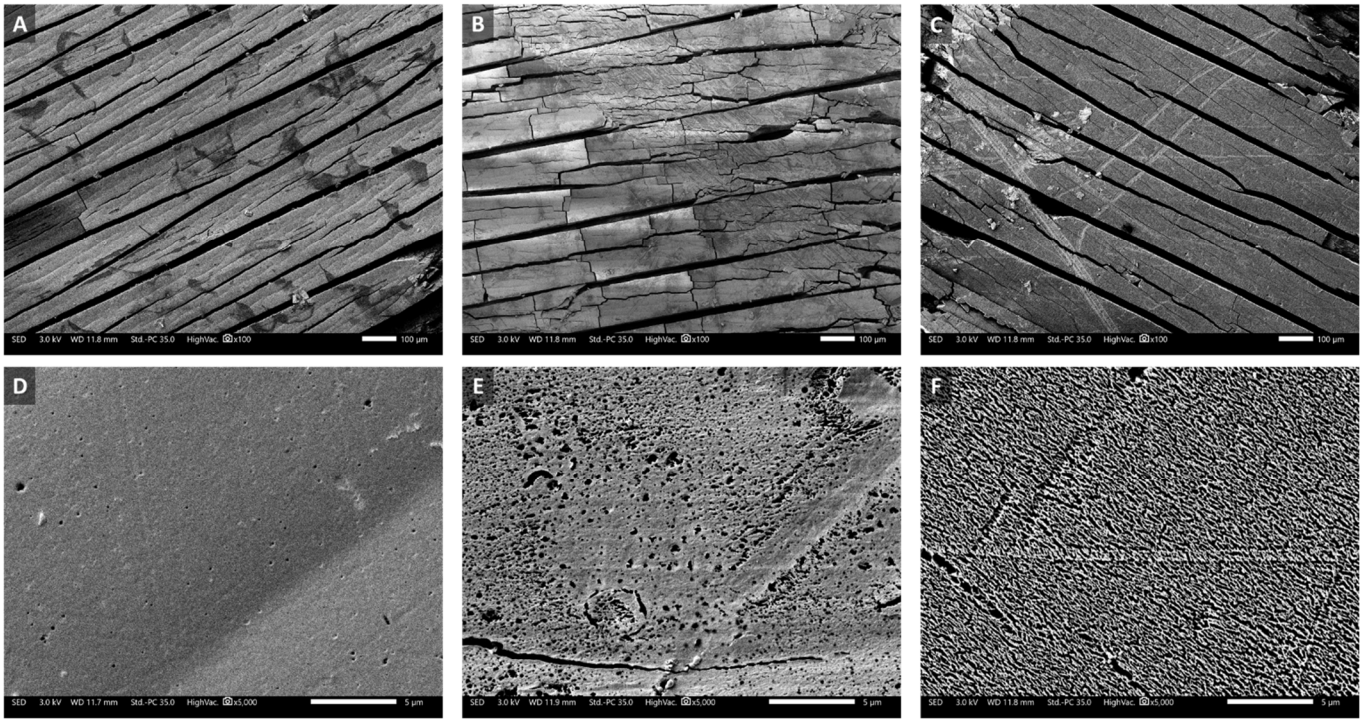

Figure 5 - Surface morphology under electron microscopy of POM-H under UV and water spray after 7 days (A and D), 14 days (B and E) and 21 days (C and F). x100 magnification on the top-row, x5000 magnification on the bottom-row

At a higher magnification (x5000), surface cracking was very limited for the POM-H after one week, but a few cavities were visible. After two weeks, more cavities appeared and after three weeks a complete surface degradation with nano-scale cracks occurred. For the POM-C, this complete surface degradation with nano-scale cracks appeared after the first week.

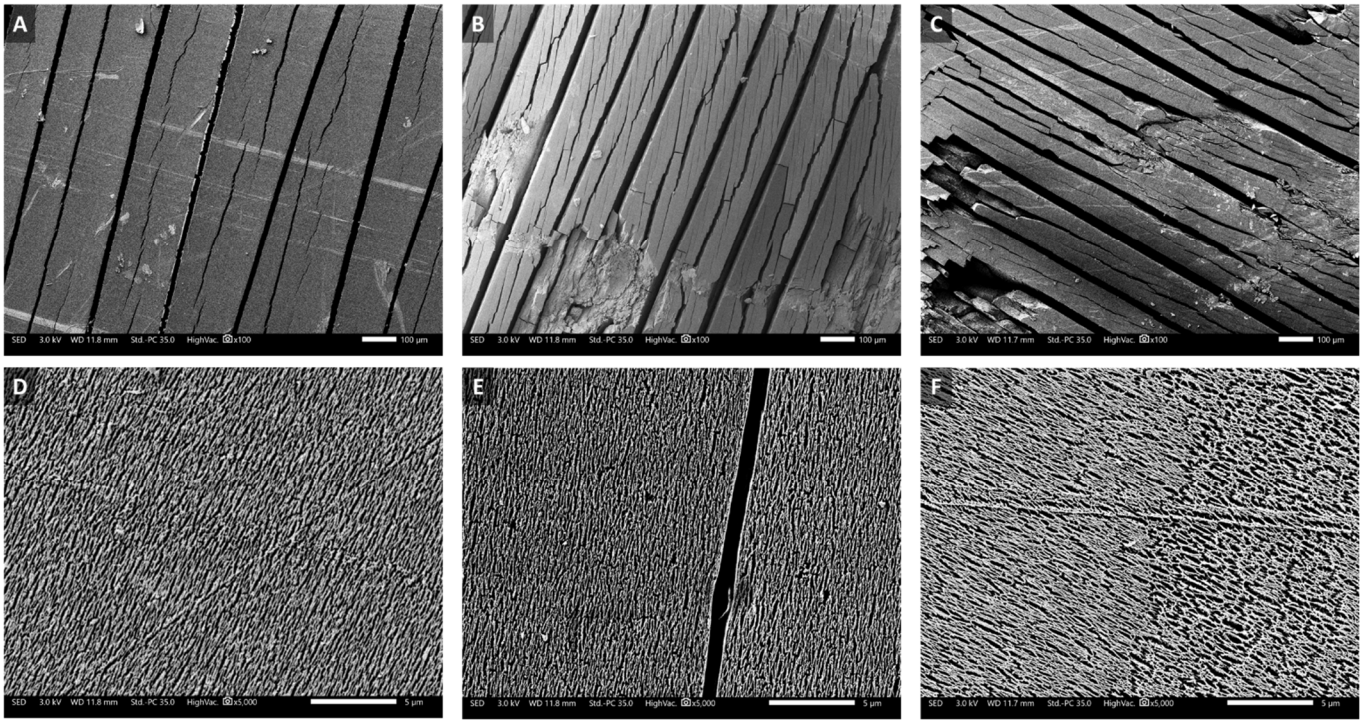

Figure 6 - Surface morphology under electron microscopy of POM-C under UV and water spray after 7 days (A and D), 14 days (B and E) and 21 days (C and F). x100 magnification on the top-row, x5000 magnification on the bottom-row

By splitting a POM sample using liquid nitrogen and observing the section, different morphologies were observed in the sample thickness (cf. Figure 6). The samples were injection molded, so a cooling gradient through the thickness is known to induce a layered structure. Indeed, Christöfl et al. have highlighted that in POM injected samples, the skin layer is a less crystalline and more amorphous zone than the bulk layer [21]. The present SEM image shows a clear separation between the outer layer and the core of the material due to the cooling gradient during injection molding. The fractured surface showed a highly fragmented top-layer (exposed to UV lamps) while the bottom-layer (not exposed) had broken in a cleaner way. Under magnification, it remained difficult to measure the crack depth: smaller cracks were 10-20 µm long, while longer cracks appeared to extend into the crystalline core layer at about 200 to 250 µm from the edge. Thus, it was assumed that the larger microplastics should be in the range of 150 to 500 µm in width. Finer cracks suggest that these fragments should continue to break into smaller pieces in the range of microns or even nanometers. Surface cracking of POM at different scales has been observed by another team that made the same assumption [19].

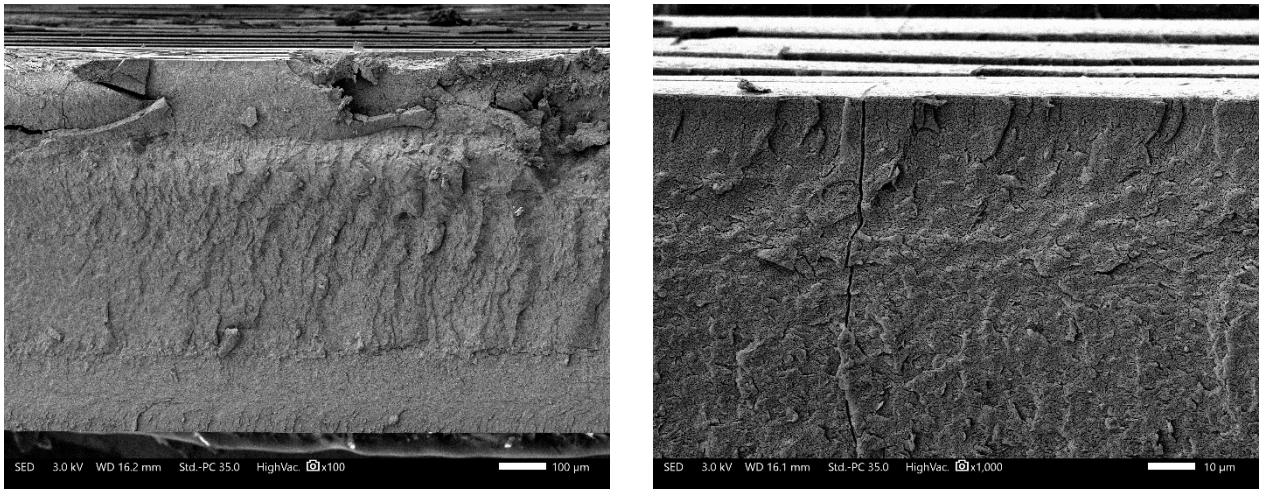

Figure 7 - Section morphology under electron microscopy of POM-C after 21 days under UV and water spray. On the left: x100 magnification, on the right: x1000.

3.2 Mechanical behavior

Tensile moduli and strengths were measured but did not show any significant evolution with exposure time. Strain at break is the most sensitive tensile property and is shown in Figure 7 for the natural conditions. Under climatic or marine conditions, the mechanical properties of both POM remained similarly stable up to 6 months. However, the strain at break decreased drastically under climatic weathering and POM became fragile and brittle at 18 months. At this stage, handling of the samples led to polymer fragmentation into microplastics. In seawater, the properties were stable up to 15 months and started to decrease slightly at 18 months. Comparatively, the mechanical properties of POM did not change during the first months of exposure. Longer exposure times were necessary to observe a significant mechanical degradation. The stability of the first month can be attributed to a seasonal effect, but more likely to an induction time of POM degradation already observed in the literature and ascribed to the consumption of stabilizing agents. Depending on temperature and oxygen pressure or concentration, this induction time was observed in mass evolution [10] and oxidation kinetics [12], [22].

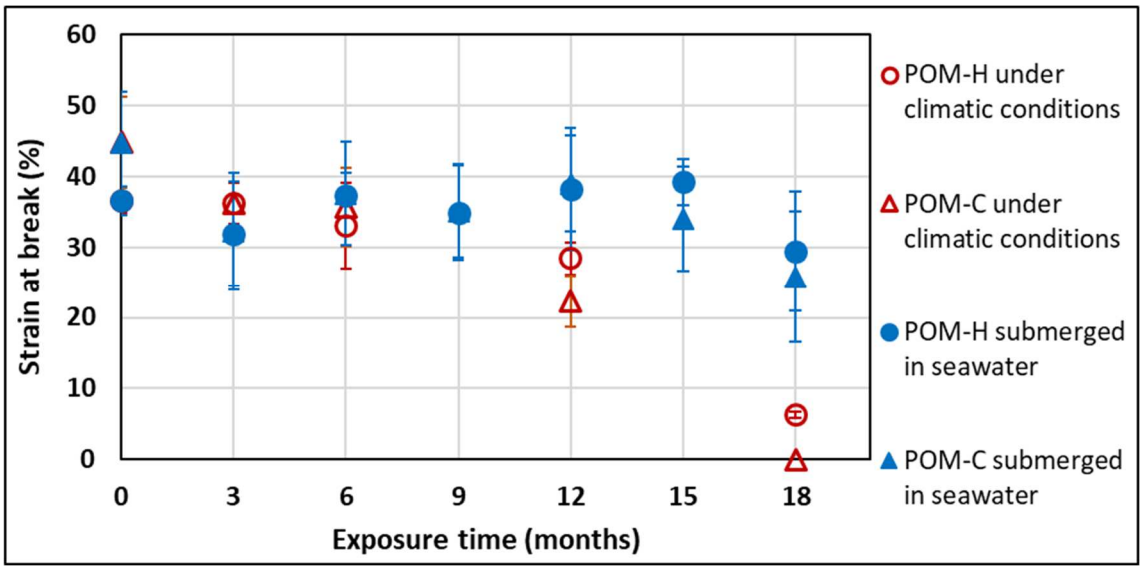

Figure 8 - Evolution of the strain at break measured by tensile test under natural weathering conditions

Under artificial UV, the induction time was not observed and Young's modulus and strength decreased steadily with exposure time (cf. Figure 8). For the strain at break, a drastic drop at seven days followed by a moderate but steady decrease up to three weeks illustrated the degradation to a very fragile and brittle state. Thus, the decrease in strain at break was attributed to POM degradation by chain scission, a well-known phenomenon in photo-oxidation and thermal oxidation mechanisms [23]. Thus, solar weathering conditions – natural or artificial – were the most detrimental conditions for POM in this study. Although POM-H was slightly stronger and stiffer in the initial state, no clear difference with POM-C was found in the evolution of mechanical properties with weathering time under these applied conditions.

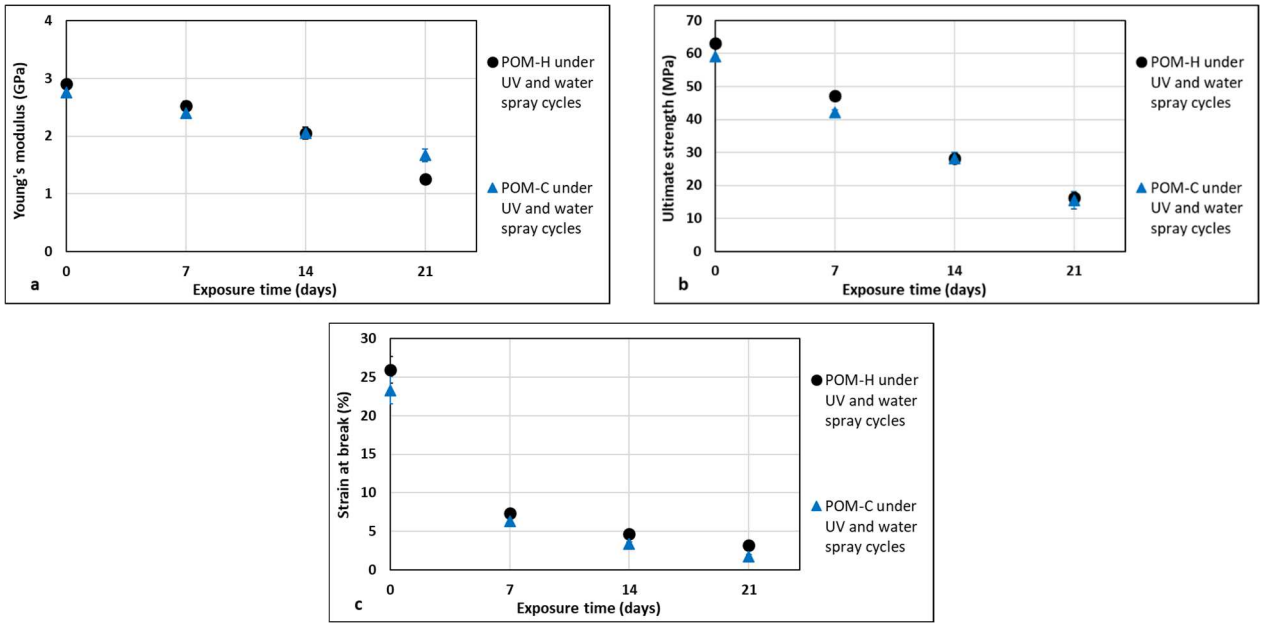

Figure 9 - Evolution of Young's modulus (a), ultimate strength (b) and strain at break (c) measured by tensile test of POM-H and POM-C under artificial weathering conditions

3.3 Polymer melting characteristics

Melting temperatures did not show any significant variation in both heating steps. As for the melting enthalpies on the first heating ramp, no significant evolution with ageing time could be reported, in congruence with the stability of the measured elastic moduli. Thus, these natural weathering conditions did not affect the crystallinity of POM-H and POM-C. In contrast, crystallinity ratios were higher in the second heating ramp but did not show significant variations with exposure time in both conditions (cf. Table 1). Thus, observed decreases in mechanical properties after climatic weathering cannot be attributed to crystallinity variations.

Table 1 - Melting temperatures, enthalpies and crystallinity measured by DSC tests (average values ± standard deviation) for the natural weathering conditions

		1st heating ramp			2nd heating ramp		
Polymer	Duration (months)	Tm (°C)	ΔHm (J.g^{-1})	$\%_{cr}$	Tm (°C)	ΔHm (J.g^{-1})	$\%_{cr}$
Under outdoor climatic conditions							
POM-H Tenac	0	181 ± 2	157 ± 9	66% ± 4%	178 ± 1	183 ± 10	77% ± 4%
	3	180 ± 0	160 ± 2	68% ± 1%	179 ± 1	181 ± 4	77% ± 2%
	6	179 ± 0	155 ± 0	66% ± 0%	178 ± 0	176 ± 1	74% ± 0%
	12	180 ± 1	146 ± 4	62% ± 2%	177 ± 1	178 ± 4	75% ± 2%
	18	177 ± 0	161 ± 6	68% ± 3%	175 ± 1	180 ± 5	76% ± 2%
POM-C Tenac	0	172 ± 0	155 ± 3	65% ± 1%	175 ± 1	180 ± 6	76% ± 3%
	3	171 ± 0	150 ± 2	63% ± 1%	172 ± 0	180 ± 2	76% ± 1%
	6	172 ± 0	151 ± 4	64% ± 2%	172 ± 0	186 ± 5	79% ± 2%
	12	172 ± 0	148 ± 4	62% ± 2%	172 ± 1	206 ± 5	87% ± 2%
	18	175 ± 3	145 ± 2	61% ± 1%	170 ± 0	183 ± 3	77% ± 1%
Submerged in seawater							
POM-H Tenac	3	180 ± 0	151 ± 5	64% ± 2%	180 ± 0	150 ± 3	63% ± 1%
	6	179 ± 0	144 ± 2	61% ± 1%	179 ± 1	160 ± 1	68% ± 0%
	12	181 ± 0	153 ± 2	65% ± 1%	181 ± 1	167 ± 6	70% ± 3%
	18	180 ± 1	159 ± 2	67% ± 1%	179 ± 0	167 ± 8	71% ± 3%
POM-C Tenac	3	173 ± 0	148 ± 1	63% ± 0%	176 ± 1	172 ± 1	73% ± 0%
	6	172 ± 2	151 ± 4	64% ± 2%	174 ± 0	174 ± 4	74% ± 2%
	12	173 ± 0	146 ± 2	62% ± 1%	176 ± 0	169 ± 1	71% ± 0%
	18	172 ± 1	150 ± 0	63% ± 0%	175 ± 0	183 ± 11	77% ± 5%

Under artificial UV, crystallinities were increased after one week of exposure, but the melting enthalpies could no longer be measured after 14 days (cf. Table 2). Other studies have evidenced a significant thermal degradation of POM after UV irradiation starting from 100°C in thermal gravimetric tests [13], [15] with formaldehyde as the main gaseous degradation product [14]. With DSC tests performed up to 200°C, this thermal degradation hinders the ability to measure enthalpies during the first heating step.

For the second heating ramp, the crystallinity ratios were substantially increased after 3 weeks for POM-H from 77% (±4%) to 94% (±9%), while POM-C was not significantly affected. This value of 94% seems odd and can reflect a DSC signal that has been disturbed by the POM thermal degradation occurring during the heating ramp. Thus, POM-H showed a greater degradation phenomenon under these artificial UV conditions,

while POM-C crystallinity remained unchanged. This can be attributed to a degradation of the amorphous part [24], or a chemi-crystallization phenomenon promoted by short chains [9]. In congruence with the POM-C stability, Archodoulaki et al. have previously demonstrated POM copolymer higher stability to oxidation compared to POM homopolymer by OIt (Oxygen Induction Time) tests [13].

Table 2 - Melting temperatures, enthalpies and crystallinity measured by DSC tests (average values ± standard deviation) for the artificial weathering conditions

		1st heating ramp			2nd heating ramp		
Polymer	Duration (days)	Tm (°C)	ΔHm (J.g^{-1})	$\%_{cr}$	Tm (°C)	ΔHm (J.g^{-1})	$\%_{cr}$
Under UV and water spray cycles							
POM-H Tenac	0	181 ± 2	157 ± 9	66% ± 4%	178 ± 1	183 ± 10	77% ± 4%
	7	176 ± 0	182 ± 1	77% ± 0%	174 ± 0	182 ± 3	77% ± 1%
	14	174 ± 1	n.d.	n.d.	173 ± 1	179 ± 2	76% ± 1%
	21	174 ± 1	n.d.	n.d.	173 ± 0	222 ± 22	94% ± 9%
POM-C Tenac	0	172 ± 0	155 ± 3	65% ± 1%	175 ± 1	180 ± 6	76% ± 3%
	7	170 ± 0	171 ± 7	72% ± 3%	171 ± 2	182 ± 3	77% ± 1%
	14	170 ± 3	n.d.	n.d.	170 ± 2	189 ± 9	80% ± 4%
	21	172 ± 2	n.d.	n.d.	169 ± 0	187 ± 7	79% ± 3%

DSC results have shown a very slight increase in crystallinity with natural weathering time and an important chemi-crystallization mechanism of POM-H under artificial UV conditions.

3.4 Surface oxidation

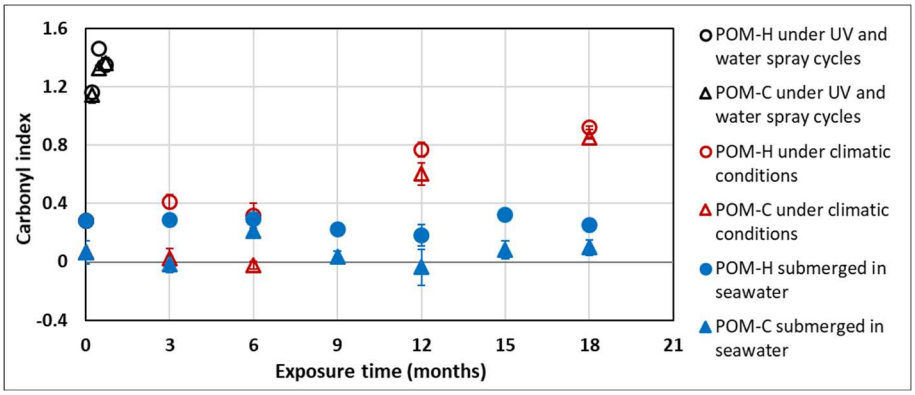

Figure 10 - Carbonyl indices as a function of exposure time in the different weathering conditions

Under climatic conditions, POM-H and POM-C carbonyl indices followed a similar trend: quite stable indices around zero in the first six months, followed by a sharp increase at 12 and 18 months between 0.8 and 1. Thus, surface oxidation seemed to occur after a certain exposure time and not immediately. Since the first six months were a fall-winter season with lower sunlight and temperatures, this evolution may be due to a seasonal effect. It may also be due to an induction time attributed to the consumption of stabilizing agents [12], [22]. In the case of seawater immersion, the carbonyl indices remained stable through the seasons revealing the absence of oxidation.

After a few weeks under artificial UV, the carbonyl indices were higher than after 18 months under natural climatic conditions, with values between 1 and 1.5. As for the mechanical property evolution, no induction time was observed.

3.5 Viscosity evolution

The complex viscosities of POM-H and POM-C are plotted in Figure 10 and 11 for climatic and seawater conditions respectively. Artificially UV-weathered samples were not plotted as rheometry tests were not possible due to strong thermal degradation during the test. Indeed, pre-oxidized POM degrades at temperatures below the melting temperature [13].

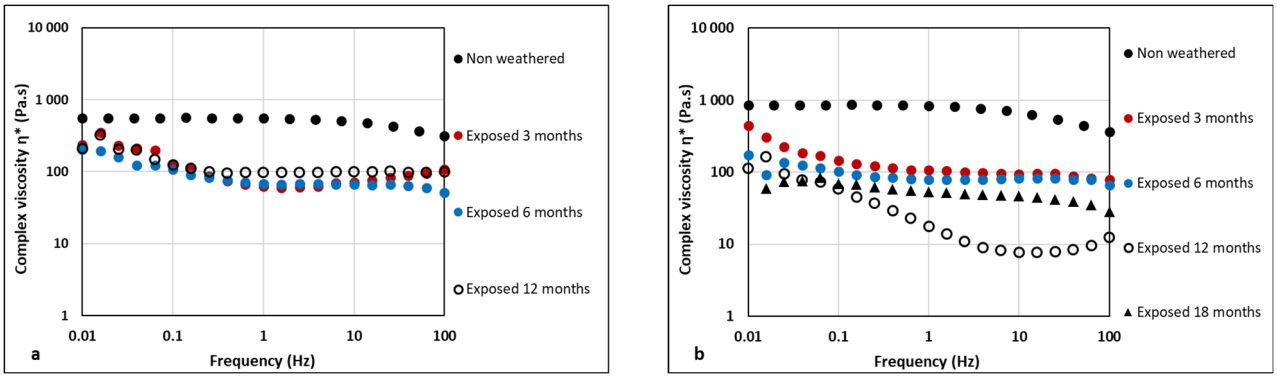

Figure 11 - Complex viscosity of POM-H (a) and POM-C (b) under climatic conditions with different exposure time

In the initial state, both POM polymers exhibited the typical polymer Newtonian plateau below 1 Hz around 800-1000 Pa.s. Under climatic conditions, the viscosities decreased sharply after 3 months but did not evolve with exposure time. The viscosities at low frequencies (0.01 to 0.1 Hz) remained close to the initial state, suggesting that the average molar masses were little affected. The rheological tests were not possible for the 18-month POM-H samples because strong thermal degradation occurred during the test with the release of a strong formaldehyde smell. Thermal oxidative degradation is known to significantly reduce POM viscosity with exposure time [23]. Since POM is known to degrade predominantly via a depolymerisation process under oxidative conditions, this phenomenon is not sufficient to significantly change the viscosity as random chain scission would (like photo-oxidized polypropylene for instance [25], [26]).

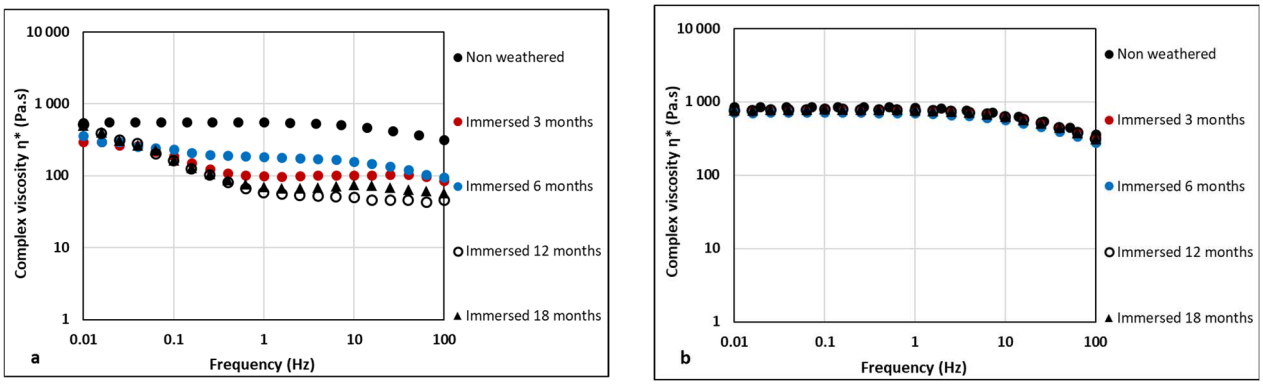

255 *Figure 12 - Complex viscosity of POM-H (a) and POM-C (b) submerged in seawater with different exposure*
256 *time*

257 When immersed in seawater, POM-H and POM-C showed different evolution. POM-H viscosity decreased
258 sharply at high frequencies but remained similar to 0.01 Hz, indicating no significant decrease in average
259 molar mass but a possible appearance of short chains. However, this trend did not correlate with the
260 evolution of the mechanical properties of POM-H in seawater. POM-C, on the other hand, did not show any
261 decrease in viscosity during its 18-months of immersion in seawater. Thus, the microstructure of POM-H
262 appeared to be altered in seawater, whereas other characterizations have shown the preservation of its
263 properties over time. The appearance of short chains or the leaching of POM-H additives in seawater could
264 explain this tendency.

265 ## 3.6 Discussion

266 When comparing the different characteristics of POM, two seem to correlate well (Pearson coefficient r = -
267 0.91): the carbonyl index and the strain at break, as shown in Figure 12. Thus, high carbonyl indices
268 correspond to low strains at break. Low carbonyl indices correspond to samples that remained mechanically
269 resistant.

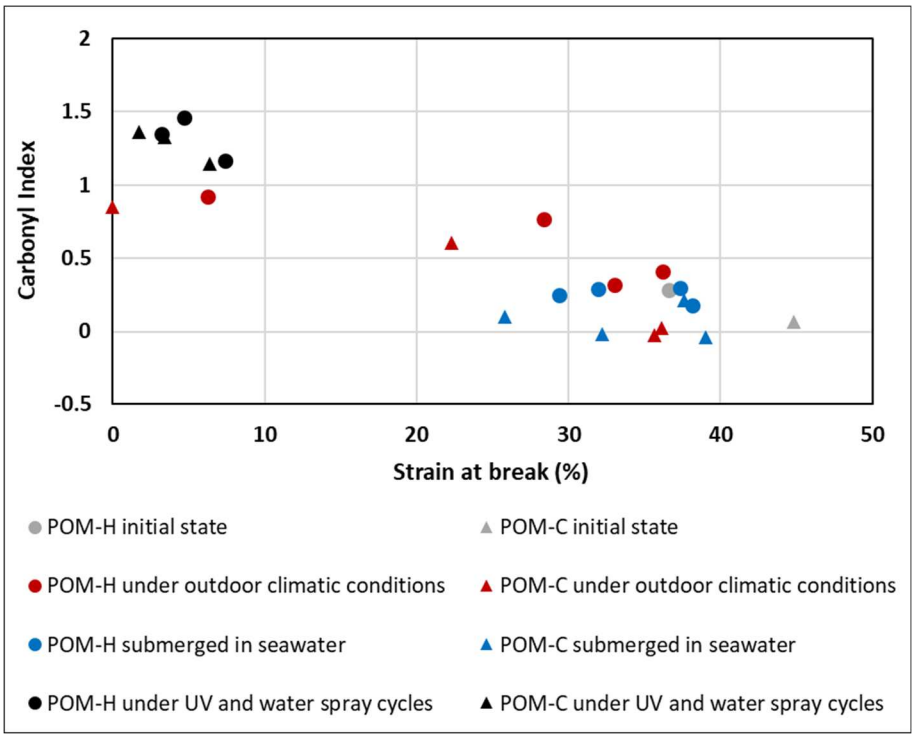

Figure 13 - Carbonyl index as a function of strain at break for all the weathering conditions at each exposure time for both POM polymers

Thus, the two distinct groups of dots suggest two stages of the POM degradation process. In the lower right portion of the graph are all the submerged samples, as well as samples aged under climatic conditions for a short period of time. At this stage, the stabilizing agents may have been consumed or the weathering conditions may not have been sufficient to significantly degrade the POM. Artificially weathered samples and highly degraded samples from climatic conditions (exposure of 18 months) are found in the upper left part of the graph. At this stage, POM were fragile and brittle, and began to fragment into microplastics. The transition between these two stages occurred very rapidly for the artificial weathering (before one week) whereas it appeared between 12 and 18 months under climatic conditions. Submerged in seawater, the degradation was too limited to make the POM polymers brittle until 18 months. From a general point of view, POM-C samples showed lower carbonyl indices in all conditions, leading to assume that POM-C is less sensitive to oxidation. Otherwise, the mechanical properties of POM-C did not show a better stability than POM-H.

4 Conclusion

In the present study, poly(oxymethylene) was investigated under different weathering conditions using physico-chemical characterization techniques. To understand how a POM macroplastic would evolve under different sets of weathering, two POM references were subjected to 18 months of climatic or marine weathering conditions or a few weeks of artificial UVB/water spray cycles. The samples were then characterized by electron microscopy, tensile tests, DSC, infrared spectroscopy and rheometry tests.

Natural climatic conditions were the most favorable conditions for POM degradation, especially under solar UV rays as evidenced by the strong fragmentation into microplastics when subjected to artificial UV cycles. The evolution of properties with exposure time was found to be non-linear under natural conditions, as opposed to artificial conditions. Highly fragmented POM samples showed fragments in the range of 150 to 500 µm wide. Finer cracks suggest that these fragments should continue to break into smaller pieces in the range of microns or even nanometers. At these dimensions, POM is unlikely to be found in surface water samples as its density of 1.4 $g.cm^{-3}$ causes it to sink. Furthermore, no significant difference was found between the POM homopolymer and the POM copolymer under the conditions studied. Since its exact composition was unknown, it was difficult to fully understand the behavior of POM. Otherwise, the possible effect of seasons was not considered here, and the duration of exposure should be extended to be able to meet the extreme level of degradation found on POM litter from the environment.

Based on this study, two degradation phases were observed. The most degraded state is when carbonyl indices are high and strain at break is low: strong POM fragmentation takes place to form microplastics, which continue to break down into nanoplastic particles as the degradation phenomenon keeps progressing. This was only observed under extreme artificial UV conditions or long natural outdoor exposure and not in seawater.

Based on these results, it can be expected that a macro or meso plastic litter in uncolored POM polymer could stay intact before producing microplastics during about one year in climatic conditions (on a beach or a river bank for instances). Several years should be necessary to completely break it down into microplastics depending on the initial size. In contrast, the POM lifespan under water is impossible to estimate as no material characteristics have been altered. So POM items are expected to remain intact after many years under water. As suggested by the Figure 13, the evolution through microplastics is strongly correlated by a highly oxidized and brittle condition, condition being likely to happen under UV exposure. Thus, it is assumed that predicting the future of POM plastic litter in the environment is a difficult task, as it will depend on its journey from land sources to the sea and finally to sediments due to its high density.

Future work should focus on the formation of microplastics, the formaldehyde release and the toxicity as a function of the degradation state in seawater as well as in freshwater. Further investigations on POM plastic materials should be extended to POM copolymers and biobased POM. Other types of engineering plastics should also be considered as they may be potentially more detrimental to fauna and flora than more studied polymers such as polypropylene, polyethylene or polystyrene.

Acknowledgments

We would like to thank the Plastic@Sea company for the fruitful discussions and Anthony Magueresse for the SEM analyzes.

References

[1] A. L. Andrady, « The plastic in microplastics: A review », *Mar. Pollut. Bull.*, vol. 119, n° 1, p. 12-22, juin 2017, doi: 10.1016/j.marpolbul.2017.01.082.

[2] P. Liu *et al.*, « Review of the artificially-accelerated aging technology and ecological risk of microplastics », *Sci. Total Environ.*, p. 144969, janv. 2021, doi: 10.1016/j.scitotenv.2021.144969.

[3] D. Gao, X. Li, et H. Liu, « Source, occurrence, migration and potential environmental risk of microplastics in sewage sludge and during sludge amendment to soil », *Sci. Total Environ.*, vol. 742, p. 140355, nov. 2020, doi: 10.1016/j.scitotenv.2020.140355.

[4] C. G. Avio, S. Gorbi, et F. Regoli, « Plastics and microplastics in the oceans: From emerging pollutants to emerged threat », *Mar. Environ. Res.*, vol. 128, p. 2-11, juill. 2017, doi: 10.1016/j.marenvres.2016.05.012.

[5] M. Kedzierski *et al.*, « Threat of plastic ageing in marine environment. Adsorption/desorption of micropollutants », *Mar. Pollut. Bull.*, vol. 127, p. 684-694, févr. 2018, doi: 10.1016/j.marpolbul.2017.12.059.

[6] M. W. Kwan So, L. D. Vorsatz, S. Cannicci, et C. Not, « Fate of plastic in the environment: From macro to nano by macrofauna », *Environ. Pollut.*, p. 118920, févr. 2022, doi: 10.1016/j.envpol.2022.118920.

[7] G. Erni-Cassola, V. Zadjelovic, M. I. Gibson, et J. A. Christie-Oleza, « Distribution of plastic polymer types in the marine environment; A meta-analysis », *J. Hazard. Mater.*, vol. 369, p. 691-698, mai 2019, doi: 10.1016/j.jhazmat.2019.02.067.

[8] A. E. Schwarz, T. N. Ligthart, E. Boukris, et T. van Harmelen, « Sources, transport, and accumulation of different types of plastic litter in aquatic environments: A review study », *Mar. Pollut. Bull.*, vol. 143, p. 92-100, juin 2019, doi: 10.1016/j.marpolbul.2019.04.029.

[9] B. Fayolle et J. Verdu, « Radiation aging and chemi-crystallization processes in polyoxymethylene », *Eur. Polym. J.*, vol. 47, n° 11, p. 2145-2151, nov. 2011, doi: 10.1016/j.eurpolymj.2011.08.003.

[10] B. Fayolle, J. Verdu, M. Bastard, et D. Piccoz, « Thermooxidative ageing of polyoxymethylene, part 1: Chemical aspects », *J. Appl. Polym. Sci.*, vol. 107, n° 3, p. 1783-1792, 2008, doi: 10.1002/app.26648.

[11] M. Bastard, « Etude de la durabilité de pièces thermoplastiques. Application au polyoxyméthylène. », PhD thesis, Arts et Métiers ParisTech, Paris, 2006.

[12] N. V. Ramirez, M. Sanchez-Soto, S. Illescas, et A. Gordillo, « Thermal Degradation of Polyoxymethylene Evaluated with FTIR and Spectrophotometry », *Polym.-Plast. Technol. Eng.*, vol. 48, n° 4, p. 470-477, avr. 2009, doi: 10.1080/03602550902725472.

[13] V.-M. Archodoulaki, S. Lüftl, et S. Seidler, « Oxidation induction time studies on the thermal degradation behaviour of polyoxymethylene », *Polym. Test.*, vol. 25, n° 1, p. 83-90, févr. 2006, doi: 10.1016/j.polymertesting.2005.08.011.

[14] S. Lüftl, V.-M. Archodoulaki, et S. Seidler, « Thermal-oxidative induced degradation behaviour of polyoxymethylene (POM) copolymer detected by TGA/MS », *Polym. Degrad. Stab.*, vol. 91, n° 3, p. 464-471, mars 2006, doi: 10.1016/j.polymdegradstab.2005.01.029.

[15] V.-M. Archodoulaki, S. Lüftl, T. Koch, et S. Seidler, « Property changes in polyoxymethylene (POM) resulting from processing, ageing and recycling », *Polym. Degrad. Stab.*, vol. 92, n° 12, p. 2181-2189, déc. 2007, doi: 10.1016/j.polymdegradstab.2007.02.024.

[16] M. M. Qayyum et J. R. White, « The effect of weathering on residual stresses and mechanical properties in injection-moulded semi-crystalline polymers », *J. Mater. Sci.*, vol. 21, n° 7, p. 2391-2402, juill. 1986, doi: 10.1007/BF01114283.

[17] J. -L. Gardette, H. -D. Sabel, et J. Lemaire, « Photooxidation of polyacetal copolymers, 1. A preliminary study of the long wavelengths photooxidation », *Angew. Makromol. Chem.*, vol. 188, n° 1, p. 113-128, 1991, doi: 10.1002/apmc.1991.051880111.

[18] H. Cottin, M.-C. Gazeau, J.-F. Doussin, et F. Raulin, « An experimental study of the photodegradation of polyoxymethylene at 122, 147 and 193 nm », *J. Photochem. Photobiol. Chem.*, vol. 135, n° 1, p. 53-64, juin 2000, doi: 10.1016/S1010-6030(00)00274-4.

[19] C.-C. Tang, Y.-T. Chen, Y.-M. Zhang, H.-I. Chen, P. Brimblecombe, et C.-L. Lee, « Cracking and Photo-Oxidation of Polyoxymethylene Degraded in Terrestrial and Simulated Marine Environments », *Front. Mar. Sci.*, vol. 9, 2022, Consulté le: 1 décembre 2022. [En ligne]. Disponible sur: https://www.frontiersin.org/articles/10.3389/fmars.2022.843295

[20] M. Deroiné, G. César, A. Le Duigou, P. Davies, et S. Bruzaud, « Natural Degradation and Biodegradation of Poly(3-Hydroxybutyrate-co-3-Hydroxyvalerate) in Liquid and Solid Marine Environments », *J. Polym. Environ.*, vol. 23, n° 4, p. 493-505, déc. 2015, doi: 10.1007/s10924-015-0736-5.

[21] P. Christöfl *et al.*, « Morphological characterization of semi-crystalline POM using nanoindentation », *Int. J. Polym. Anal. Charact.*, vol. 26, n° 8, p. 692-706, nov. 2021, doi: 10.1080/1023666X.2021.1968122.

[22] M. B. Neiman, *Aging and Stabilization of Polymers*, 1/2012 éd. Springer Verlag GmbH, 2012. Consulté le: 8 décembre 2022. [En ligne]. Disponible sur: https://www.ernster.com/fr/detail/ISBN-9781461585510/Neiman-M-B/Aging-and-Stabilization-of-Polymers

[23] S. Lüftl, V.-M. Archodoulaki, M. Glantschnig, et S. Seidler, « Influence of coloration on initial material properties and on thermooxidative ageing of a polyoxymethylene copolymer », *J. Mater. Sci.*, vol. 42, n° 4, p. 1351-1359, févr. 2007, doi: 10.1007/s10853-006-1217-y.

[24] F. Julienne, F. Lagarde, et N. Delorme, « Influence of the crystalline structure on the fragmentation of weathered polyolefines », *Polym. Degrad. Stab.*, vol. 170, p. 109012, déc. 2019, doi: 10.1016/j.polymdegradstab.2019.109012.

[25] A. E. Delorme *et al.*, « The life of a plastic butter tub in riverine environments », *Environ. Pollut.*, vol. 287, p. 117656, oct. 2021, doi: 10.1016/j.envpol.2021.117656.

[26] L. Soccalingame, D. Perrin, J.-C. Bénézet, S. Mani, E. Richaud, et A. Bergeret, « Reprocessing of artificial UV-weathered wood flour reinforced polypropylene composites », *Polym. Degrad. Stab.*, vol. 120, p. 313-327, oct. 2015, doi: 10.1016/j.polymdegradstab.2015.07.013.